RESEARCH ARTICLE

DOI: 10.54926/jnamt.2025.2518

J Nav Architect Mar Technol 2025;227(1):64-73

Wave-Induced Force Modeling on a Monopile Foundation at Gökçeada Using Spectral and Diffraction-Based Approaches

Deniz Bayraktar Bural

İstanbul Technical University Faculty of Naval Architecture and Ocean Engineering, Department of Shipbuilding and Ocean Engineering, İstanbul, Türkiye

To cite this article: D. Bayraktar Bural. Wave-induced force modeling on a monopile foundation at gökçeada using spectral and diffraction-based approaches. *J Nav Architect Mar Technol*. 2025;227(1):64-73.

Received: 05.05.2025 - **Revision Requested:** 14.06.2025 - **Accepted:** 10.07.2025 - **Publication Date:** 18.07.2025

Abstract

This study presents a numerical framework to reconstruct long-term wave-induced force histories on monopile foundations supporting offshore wind turbines in data-limited, fetch-limited marine environments. The methodology is demonstrated for the northeastern Aegean Sea near Gökçeada, where in-situ wave measurements are limited or not readily available. The objective is to model the wave-induced forces acting on offshore monopile-supported wind turbines under irregular sea states. By combining site-specific spectral wave data with diffraction-based force estimation, the study provides a detailed assessment of hydrodynamic load contributions across the frequency domain, offering critical insights for offshore wind energy infrastructure in the Northern Aegean Sea. A site-specific JONSWAP spectrum is constructed using a 10-year reanalysis dataset to characterize the local sea state. Wave loading on the monopile is estimated using MacCamy-Fuchs diffraction theory, which captures frequency-dependent hydrodynamic effects for large-diameter cylindrical structures. To ensure theoretical consistency, spectral components outside the applicable range are excluded with minimal energy loss. The resulting force spectrum is transformed into the time domain using inverse Fourier techniques with randomized phase, yielding a representative wave force signal for time-domain analysis. To assess extreme loading conditions, a statistical extreme value analysis is performed using threshold-based fitting. The proposed framework enables realistic wave load simulation in coastal regions lacking field measurements and supports applications such as fatigue assessment, reliability analysis, and offshore wind turbine design in semi-enclosed seas.

Keywords: Offshore wind turbines, MacCamy-Fuchs diffraction theory, wave-induced forces, JONSWAP spectrum, monopile foundations

1. Introduction

Offshore wind energy has become an increasingly vital component of sustainable energy strategies worldwide, driven by the urgent need to transition to renewable energy sources. In this context, Turkey, particularly the Aegean and Marmara Seas, holds significant offshore wind energy potential [1]. Among these regions, Gökçeada stands out as a promising site due to its strong wind resources and favorable water depths for offshore wind turbine installations [2,3]. Prior optimization studies, such as those by Şişbot et al. [4], have demonstrated that carefully planned turbine placement in Gökçeada can enhance energy production while maintaining structural and environmental feasibility. Recent technical feasibility assessments have further confirmed the suitability of the site for offshore wind development [5].

While wind energy availability is crucial for site selection, offshore structural design requires a thorough understanding of wave conditions, particularly in light of the growing

Address for Correspondence: Deniz Bayraktar Bural, İstanbul Technical University Faculty of Naval Architecture and Ocean Engineering, Department of Shipbuilding and Ocean Engineering, İstanbul, Türkiye
E-mail: bayraktard@itu.edu.tr
ORCID ID: orcid.org/0000-0002-4541-9089

frequency of extreme weather events associated with climate change and the region-specific design criteria emphasized in offshore wind standards [6]. Accurate knowledge of wave height, peak period, and wave direction is fundamental for coastal and offshore engineering applications. Over the past decade, numerous studies have leveraged reanalysis data and numerical modeling to characterize wave climates and their variability across different maritime regions.

Sartini et al. [7] conducted a detailed analysis of 32 years of hindcast wave data in the North Tyrrhenian Sea, extracting critical parameters such as significant wave height, peak period, and dominant wave direction (VMDR). Similarly, Pillai et al. [8] analyzed long-term wave trends along the Emilia-Romagna coast, validating numerical results against field observations to improve nearshore wave climate representation. Ibrahim et al. [9] further highlighted an increasing trend in significant wave heights along the Mediterranean coastline, underscoring the growing influence of climatic shifts on coastal environments.

Understanding these evolving wave climates is essential not only for coastal resilience but also for the structural integrity of offshore wind turbines. The impact of extreme wave conditions on offshore foundations has been widely investigated through the application of wave spectra models. For instance, Fan [10] emphasized the need for accurate design wave height estimations to ensure structural resilience during extreme events such as typhoons. Li et al. [11] complemented these findings with experimental data on the hydrodynamic forces exerted on curved vertical structures, providing valuable insights into wave-structure interactions under varying sea states.

Recent advances in global climate reanalysis datasets, such as ERA5 and ECMWF products, have further enhanced the ability to characterize wave behavior on both regional and global scales. Napitupulu et al. [12] demonstrated how meteorological conditions strongly influence the spatiotemporal variability of significant wave heights, as observed in the Riau Archipelago, reinforcing the importance of accurate wave modeling for structural and navigational safety.

Given that real sea states consist of multiple interacting wave components, spectral analysis offers a more realistic representation of wave loads acting on marine structures compared to deterministic approaches. The design and stability of offshore wind turbines, particularly those supported by monopile foundations, depend critically on the accurate estimation of wave-induced forces under such irregular sea states [13]. Wave spectrum models provide insight into how energy is distributed across different frequency components, influencing the dynamic response of structures [14,15].

In this study, the JONSWAP spectrum has been selected to model the wave environment at Gökçeada. Originally developed for the North Sea, the JONSWAP spectrum remains highly applicable to semi-enclosed and fetch-limited environments when properly adapted. Recent studies support this approach: Vlachogiannis et al. [16] demonstrated the effectiveness of the JONSWAP model in predicting wave energy in shallow coastal areas when site-specific calibration is performed. Similarly, Spanoudaki et al. [17] confirmed that JONSWAP-based frameworks successfully capture the spatiotemporal variability of wave fields in the Aegean Sea. The importance of carefully selecting spectral parameters, particularly the peak enhancement factor γ, to accurately represent local conditions is also emphasized in sensitivity analyses by Barbariol et al. [18] and Xie et al. [19]. These findings collectively justify the application of the JONSWAP model in the Aegean Sea for reliable wave force estimation.

To further validate the fetch-limited characterization of the Gökçeada offshore site, wave climate data from the CMEMS were analyzed. The VMDR was compared with ERA5 wind data, confirming that the wave field in the region is primarily wind-driven with limited swell influence. The semi-enclosed nature of the Aegean Sea supports the classification of the study area as a fetch-limited environment, consistent with the modeling assumptions.

Based on these environmental conditions, wave force estimation for the monopile foundation at Gökçeada is approached using diffraction theory. When the monopile diameter is large relative to the incident wavelength, diffraction effects dominate the hydrodynamic response. In this study, MacCamy-Fuchs diffraction theory is employed to estimate wave-induced forces on the monopile. The validity of this approach is supported by key non-dimensional parameters: the diameter-to-wavelength ratio ($D/L>0.2$) and the water depth-to-wavelength ratio ($h/L>0.5$) indicate diffraction dominance, while the depth-to-diameter ratio ($h/D>1$) further supports the theoretical framework under the local site conditions.

The objective of this study is to model the wave-induced forces acting on offshore monopile-supported wind turbines at Gökçeada under irregular sea states. By combining site-specific spectral wave data with diffraction-based force estimation methods, the study provides a detailed assessment of hydrodynamic load contributions across the frequency domain, offering critical insights for the design and structural analysis of offshore wind energy infrastructure in the Northern Aegean Sea.

2. Site Characteristics and Data Collection

2.1. Location of the Study Area

This study focuses on the offshore region surrounding Gökçeada, the largest island in Türkiye, located in the northeastern Aegean Sea (~40.2 °N, 25.9 °E). The site offers technical suitability for offshore wind development due to its exposure to strong, persistent winds-particularly the seasonal Etesians that shape the local wave climate.

Figure 1 shows a screenshot from the CMEMS interface, where the island of Gökçeada is clearly labeled. The blue-shaded region indicates the spatial coverage of the available reanalysis wave data, while the black rectangle outlines the coordinate bounds used for data extraction. These bounds include the selected wind turbine location and are consistent with the spatial resolution of the CMEMS product.

Bathymetric data [20] from the CMEMS indicate an average water depth of ~48.3 m at the intended turbine site, supporting the use of fixed-bottom monopile foundations. The relatively uniform seabed and fetch-limited wave conditions justify the application of spectral wave modeling to estimate hydrodynamic forces.

2.2. Wave Climate and Wind Data

Wave climate data for the study area were obtained from the Copernicus Marine Service dataset (MEDSEA_MULTIYEAR_WAV_006_012), which provides a high-resolution hindcast of wave conditions in the Mediterranean Sea. The dataset has a spatial resolution of approximately 1/24° (~4.6 km) and covers the period from January 31, 2013, to May 31, 2023. The primary wave parameters extracted include significant wave height H_s, peak wave period T_p, and mean wave direction (VMDR), which are essential for characterizing the hydrodynamic environment of the Gökçeada offshore site.

Although no *in situ* buoy data are available directly offshore of Gökçeada, the Copernicus wave parameters have undergone extensive validation across the Mediterranean basin. According to the Product Quality and Validation Report [20] the modeled significant wave heights show strong agreement with buoy and satellite measurements, with root-mean-square errors (RMSE) of 0.25-0.35 m and correlation coefficients exceeding 0.90 in the Aegean region. Mean biases were typically below 0.1 m. These performance metrics confirm the reliability of Copernicus-derived wave parameters and justify their use in site-specific modeling where direct measurements are unavailable.

Given the region's semi-enclosed geometry and dominant wind-wave alignment, the Aegean Sea is considered fetch-limited. To describe the spectral distribution of wave energy at the site, a JONSWAP spectrum was developed using 10 years of reanalysis data. The long-term mean significant wave height of this data is approximately 0.54 m corresponds to Beaufort Force 4 (Moderate Breeze), providing a practical reference for the typical sea state. Details regarding the spectral formulation, parameter calibration, and validation procedures are provided in Section 3.1.

2.3. Wind Turbine and Monopile Design

The offshore wind turbine considered in this study is assumed to be supported by a monopile foundation, which is the most widely adopted substructure type for fixed-bottom offshore wind farms. Monopiles are preferred in moderate water depths (up to approximately 50 m) due to their structural simplicity, robustness, and cost-effectiveness.

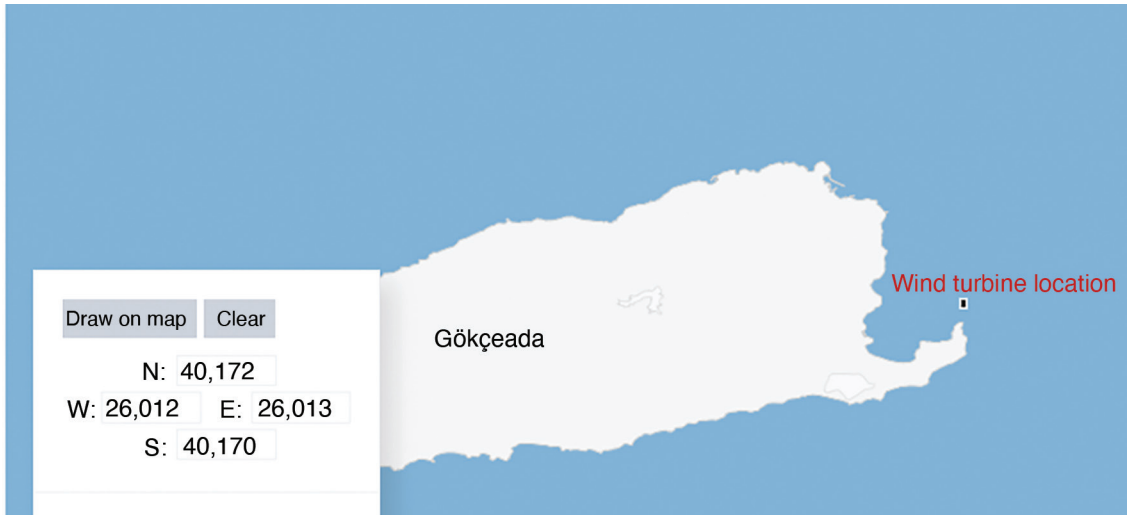

Figure 1. Screenshot from the Copernicus Marine Environment Monitoring Service, showing the study area near Gökçeada in the northeastern Aegean Sea. The blue-shaded region indicates reanalysis data coverage, and the black rectangle marks the coordinate bounds used for wave data extraction, including the wind turbine location.

A monopile diameter of D=2.5 m was selected for this study as shown in Figure 2, representing a practical dimension for offshore wind installations in similar bathymetric conditions. This diameter was directly incorporated into the diffraction-based wave force estimation using MacCamy-Fuchs theory to ensure accurate representation of wave-structure interaction effects. The analysis focuses exclusively on hydrodynamic loading induced by waves and does not consider the structural response of the wind turbine or aerodynamic forces associated with rotor operation.

Although turbine-specific aspects such as control systems, tower dynamics, or power generation are beyond the scope of this work, the computed wave-induced force signal is statistically analyzed to evaluate monthly variability, force magnitude distributions, and return-level estimates using a Peak Over Threshold (POT) approach fitted with a Generalized Pareto Distribution (GPD).

3. Methodology

The methodological framework of this study follows a structured approach to estimating wave-induced forces on the monopile foundation, incorporating site-specific wave conditions and diffraction-based force estimation. The overall procedure, from spectral input construction to time-domain force reconstruction, is summarized in Figure 3.

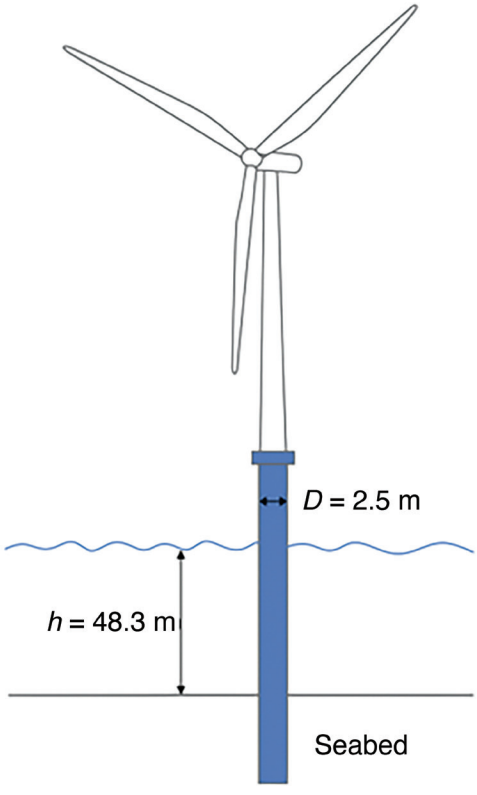

Figure 2. Schematic representation of the monopile-supported offshore wind turbine configuration.

The workflow begins with the acquisition of 10 years of reanalysis data for significant wave height (H_s), peak wave period (T_p), and mean wave direction (VMDR) from the Copernicus Marine Service. These parameters are used to construct a JONSWAP wave spectrum. The peak enhancement factor (γ) is selected adaptively based on the mean H_s, and the spectral width parameter (σ) is applied according to the standard JONSWAP formulation. The spectrum is then validated by comparing the estimated significant wave height ($H_{s,est}$) with the observed mean ($H_{s,mean}$), and an α-correction is applied to align spectral energy with reanalysis-based observations. To ensure the validity of MacCamy-Fuchs theory, a filtering step is applied to exclude spectral components where $ka>3$, and an energy retention check is performed. Spectral band contribution analysis is also conducted to quantify energy content in low, mid, and high frequency ranges.

Wave loading on the monopile is evaluated using MacCamy-Fuchs diffraction theory, which provides a frequency-dependent force transfer function suitable for vertical circular cylinders.

The wave-induced force contributions per frequency, obtained by applying the MacCamy-Fuchs transfer function to the site-specific JONSWAP spectrum, are numerically integrated over the retained frequency range to compute the total force in the frequency domain. This approach-combining a physically consistent diffraction model with validated spectral inputs-follows established practices in offshore hydrodynamic force estimation.

To evaluate the effects of irregular wave loading over time, a time-domain force signal is reconstructed using the inverse fast Fourier transform (IFFT) of the force spectrum,

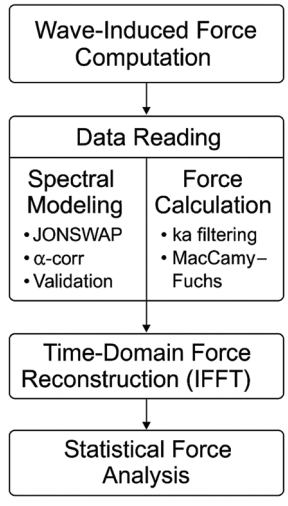

Figure 3. Computational workflow for modeling and reconstructing wave-induced forces.

generated by combining spectral magnitudes with randomly assigned phase values. This step enables the modeling of realistic, time-varying wave-induced loads acting on the monopile. The reconstructed signal is then subjected to statistical evaluation, including summary metrics such as mean, standard deviation, and percentiles, along with extreme value analysis based on the POT method. In this approach, force values exceeding the 95th percentile threshold are extracted and fitted to a GPD to estimate rare-event return levels. Further technical details related to wave spectrum formulation, diffraction theory, and numerical implementation are provided in subsequent sections. This methodological framework enables the generation of realistic, site-adapted force histories under irregular sea states and forms the basis for the statistical evaluations presented in Section 4.

3.1. Wave Spectrum Model Selection

To verify the fetch-limited nature of the study site, VMDRs extracted from the Copernicus Marine dataset were compared with prevailing wind directions from the ERA5 reanalysis product. The strong correlation between wind and wave directions, combined with the semi-enclosed geometry of the Aegean Sea, confirms that local wind forcing dominates wave generation, with negligible swell contribution. This finding justifies the use of the JONSWAP model.

A site-specific JONSWAP spectrum was then constructed using significant wave height (H_s) and peak period (T_p) values obtained from the reanalysis dataset. The spectral energy density $S(f)$ was computed according to Equation 1:

$$S(f) = \alpha g^2 f^{-5} \exp\left(-\frac{5}{4}\left(\frac{f_p}{f}\right)^4\right) \gamma^{\exp\left(-\frac{(f-f_p)^2}{2\sigma^2 f_p^2}\right)} \quad (1)$$

where α is a scaling parameter for spectral energy, f is the wave frequency in Hz, f_p is the peak frequency, g is the gravitational acceleration, σ is the spectral width parameter, and γ is the peak enhancement factor.

The peak enhancement factor γ was set to 1.8, consistent with the original JONSWAP formulation for moderately developed seas [21]. Although γ can range between 1 and 7 depending on wind and fetch conditions, values between 1.5 and 3 are typically used in engineering applications. The selected value was validated by comparing the modeled significant wave height $H_{s,est}$ with the observed mean $H_{s,mean}$ confirming the physical consistency of the spectrum.

The spectral width parameter σ was defined piecewise based on frequency relative to the spectral peak, as shown in Equation (2):

$$\sigma = \begin{cases} 0.07 \text{ for } f \leq f_p \\ 0.09 \text{ for } f > f_p \end{cases} \quad (2)$$

This asymmetric formulation reflects the structure of developing wind seas and was directly implemented in the numerical model.

To ensure consistency between the modeled spectrum and the observed wave energy, the spectral scaling coefficient α was iteratively adjusted so that the significant wave height estimated from the JONSWAP energy spectrum matched the long-term mean value obtained from the reanalysis dataset. This was performed using the standard relationship in Equation (3):

$$H_{s,\text{ estimated}} = \sqrt{16 \int S(f) df} \quad (3)$$

The final corrected spectrum was validated by comparing its peak frequency and total energy with reanalysis statistics. This validation was implemented using an in-house MATLAB code, and alignment was confirmed numerically with convergence of $H_{s,est}$ to $H_{s,mean}$=0.54 m.

As shown in Figure 4, the corrected spectrum exhibits a sharp peak around 0.34 Hz and steep decay at higher frequencies-characteristic of wind-driven waves in fetch-limited conditions.

This validated spectrum was used as input for wave force estimation. To ensure theoretical consistency within the MacCamy-Fuchs-based diffraction model [22], spectral components with non-dimensional wave number $ka>3$ were excluded.

3.2. Diffraction Theory for Wave Forces

The calculation of wave-induced forces on the monopile foundation is based on diffraction theory, which is appropriate for structures with large diameter-to-wavelength ratios.

To model wave diffraction around a vertical circular cylinder, the MacCamy-Fuchs linear diffraction theory [22] is applied. This approach defines a frequency-dependent transfer function $H_f(f)$ which modifies the hydrodynamic force according to diffraction behavior.

The wave-induced force contribution per frequency is then computed using Equation (4):

$$F(f) = \rho g D H_f S(f) \quad (4)$$

These per-frequency force contributions form the basis for calculating the total hydrodynamic load on the monopile. The integration of these contributions over the valid frequency range-along with the application of ka filtering and energy retention checks-is described in Section 3.3.

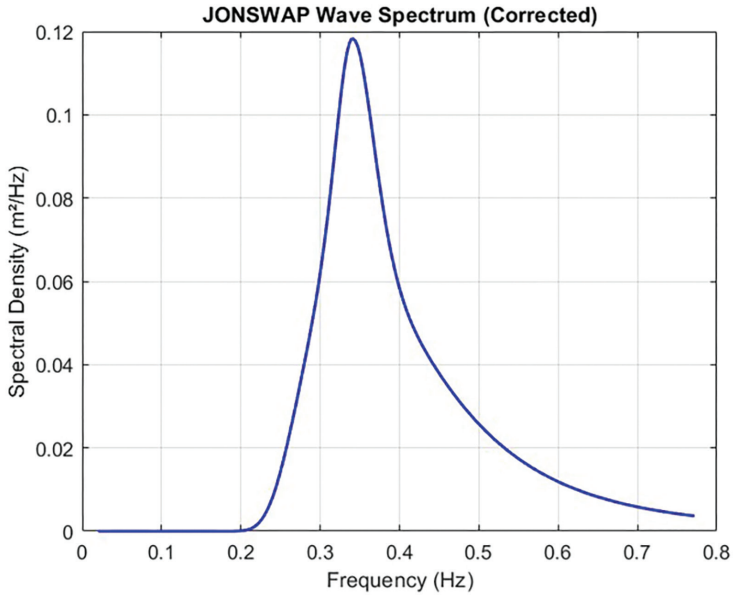

Figure 4. Corrected JONSWAP spectrum constructed from Copernicus reanalysis data for the Gökçeada offshore site, showing peak energy near 0.34 Hz under fetch-limited sea state conditions.

3.3. Numerical Implementation

The numerical implementation of MacCamy-Fuchs diffraction theory involves several computational steps to estimate wave-induced forces on the monopile foundation based on the JONSWAP spectrum. First, the wave number k is computed for each frequency by solving the linear wave dispersion relation given in Equation (5):

$$\omega^2 = gk\tanh(kh) \tag{5}$$

where $\omega = 2\pi f$ is the angular frequency and h is the water depth. This non-linear equation is solved numerically using a root-finding method with an initial guess based on deep-water approximation.

The transfer function H_f is computed using the MacCamy-Fuchs diffraction formulation for a vertical circular cylinder, as defined in Equation (6):

$$H_f = \left|1 - \frac{2J_1(kD/2)}{(kD/2)J_0(kD/2)}\right| \tag{6}$$

Here, J_0 and J_1 are Bessel functions of the first kind (orders 0 and 1), k is the wave number, and D is the diameter of the monopile. To prevent numerical instabilities and non-physical amplification in long waves, the transfer function is capped at an upper limit of $H_f = \min(H_f, 2)$. This cap reflects theoretical upper bounds found in classical diffraction theory [23].

For each frequency component, the wave-induced force contribution is calculated by multiplying the diffraction-based transfer function $H_f(f)$, the monopile diameter D and the spectral energy density $S(f)$. This computation captures the contribution of each frequency in the wave spectrum to the total hydrodynamic loading on the structure.

The total wave-induced force in the frequency domain is then obtained by numerically integrating these contributions using the trapezoidal rule, as shown in Equation (7):

$$F_{\text{total}} = \int \rho g D H_f S(f) df \tag{7}$$

This integration is performed over the valid frequency range defined by the diffraction theory limits.

Since MacCamy-Fuchs theory is applicable only when the non-dimensional wave number satisfies $ka \leq 3$, a filtering step is applied to enforce this condition, as stated in Equation (8):

$$ka = k\frac{D}{2} \leq 3 \tag{8}$$

Frequency components that do not satisfy this constraint are excluded to preserve the theoretical validity of the model.

To assess the effect of this filtering, a spectral energy retention check is performed. The total spectral energy before filtering is computed using Equation (9):

$$E_{all} = \int_{f_{min}}^{f_{max}} S(f) df \tag{9}$$

and the retained spectral energy, considering only frequencies within the valid set $F_{valid} \subset [f_{min}, f_{max}]$ is calculated as in Equation (10):

$$E_{retained} = \int S(f)df \quad (10)$$

The energy retention ratio is then determined from Equation (11):

$$Retention\ Ratio = 100\frac{E_{retained}}{E_{all}}(\%) \quad (11)$$

In this study, the retained energy after filtering exceeds 97%, indicating that the removal of high-frequency components has a negligible effect on the physical accuracy of the wave force computation.

All numerical procedures-including the computation of wave numbers via the dispersion relation, evaluation of the MacCamy-Fuchs transfer function, spectral energy filtering, numerical integration of force components, and time-domain reconstruction using IFFT with randomized phases-were implemented using an in-house MATLAB code. Built-in functions such as *fsolve*, *fft*, and *gpfit* were employed during relevant stages of the analysis.

4. Results and Discussion

This section presents the outcomes of the wave force modeling for the monopile-supported wind turbine in the Gökçeada offshore region. Using frequency-domain force components developed in Section 3, a time-varying wave-induced load signal was reconstructed to analyze load variability across the simulation period. These results were further processed to derive design-relevant statistics.

4.1. Time-Domain Wave Force Reconstruction

The wave force acting on the monopile was reconstructed in the time domain from frequency components obtained using the calibrated site-specific wave spectrum described in Section 3.1. The final spectral parameters yielded a significant wave height of H_s=0.5439 m, with a peak frequency of f_p=0.3407 Hz and corresponding peak period of T_p=2.935 s, representing typical sea conditions at the Gökçeada site.

To ensure model validity, the spectral force was truncated using the $ka \leq 3$ criterion described in Section 3.3, limiting energy loss to 2.51% and preserving the dominant hydrodynamic content. An IFFT with randomized phase angles was applied to reconstruct the time-varying force signal $F(t)$. The resulting record, shown in Figure 5, spans the entire 10-year simulation and captures both high-frequency variability and long-term modulations in wave loading. Although the applied diffraction model provides frequency-dependent amplitudes, conversion to the time domain was essential to evaluate load fluctuations, extreme values, and fatigue-relevant patterns that cannot be captured in the frequency domain alone.

A statistical comparison was performed between the frequency-domain force spectrum and the reconstructed time-domain signal obtained via IFFT with randomized phase. The frequency-domain force exhibited a standard deviation of 0.03 N and an RMS of 0.05 N, while the time-domain force signal yielded a standard deviation and RMS of 321.27 N. This apparent discrepancy arises from the inherent differences in how energy is distributed in the spectral versus time domains. The frequency-domain values are expressed per unit frequency (N²/Hz) and represent the square root of the integrated spectral force density. In contrast, the time-domain RMS force reflects the full amplitude of instantaneous loading over the reconstructed signal, normalized over time. The use of randomized phase in the IFFT ensures that the energy content is preserved, even though peak values differ

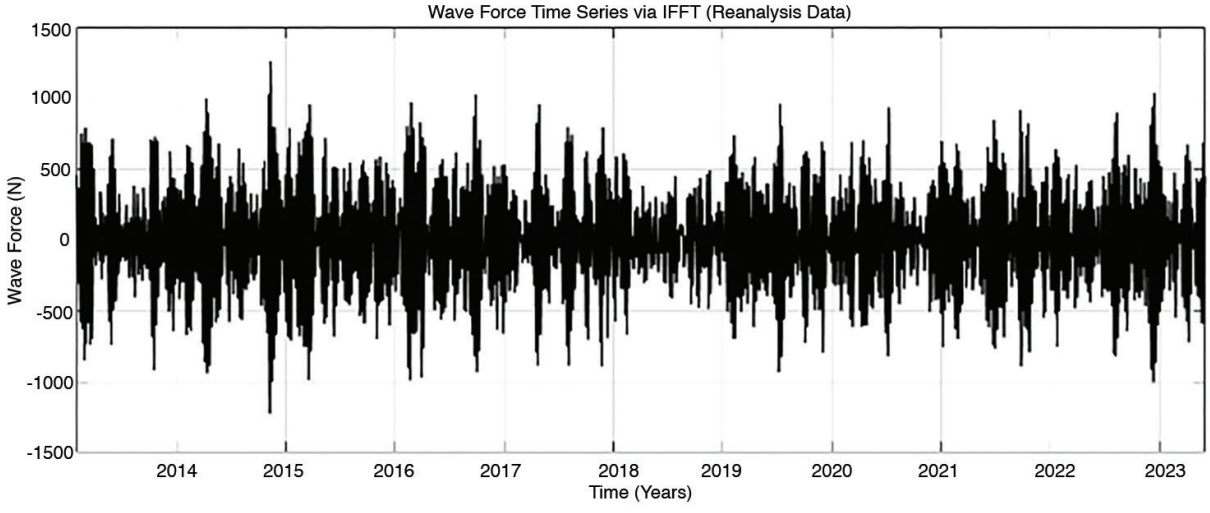

Figure 5. Reconstructed time-domain wave force signal via IFFT using site-specific JONSWAP spectrum, showing 10 years of irregular loading conditions.

substantially. Both metrics are valid within their respective domains and confirm the statistical representativeness of the reconstructed force signal. The reconstructed force time series, therefore, preserves the desired energy distribution for long-term statistical analyses and is considered suitable for further design load evaluations, including time-domain fatigue analysis, spectral bandwidth evaluation, and temporal clustering of load peaks, which cannot be assessed in the frequency domain alone.

4.2. Design Load Characterization

The reconstructed time-domain wave-induced force signal was statistically evaluated to extract load characteristics relevant for the structural design of a monopile-supported offshore wind turbine. As illustrated in Figure 6, the histogram of the reconstructed force signal reveals a near-symmetric distribution centered around zero, capturing the stochastic nature of irregular wave loading in the northeastern Aegean Sea. The force time series exhibited a maximum value of 1259.08 N, a minimum of -1226.58 N, and a standard deviation of 321.27 N. The mean value was effectively zero (-0.00 N), confirming the absence of a net directional bias in the long-term wave forcing. The histogram reveals that more than 99% of force amplitudes fall within ±3 standard deviations, indicating a bounded, stable force regime consistent with stochastic wave behavior. These results reflect realistic amplitude variability and confirm the suitability of the reconstructed signal for dynamic analysis.

To estimate extreme wave-induced loads, the POT method was applied using the 95th percentile of the reconstructed force signal as the threshold (u). This resulted in 519 exceedance values ($x>u$), which were fitted to a GPD. The cumulative distribution function of the GPD is given in Equation (12), and the corresponding return level expression is shown in Equation (13). The shape k and scale σ parameters of the GPD were estimated using MATLAB's built-in function *gpfit*, which applies maximum likelihood estimation to the exceedance data. For this study, the fitted parameters were k=0.0809 and σ=83.54 N. Using the estimated parameters and the annual rate of exceedance λ, the 50-year return force was calculated as 1351.7 N based on Equation (13).

$$F(x) = \begin{cases} 1 - \left(1 + \frac{k(x-u)}{\sigma}\right)^{-1/k} & \text{if } k \neq 0 \\ 1 - exp\left(-\frac{x-u}{\sigma}\right) & \text{if } k = 0 \end{cases} \quad \text{for } x > u \qquad (12)$$

$$z_T = u + \frac{\sigma}{k}[(T \cdot \lambda)^k - 1] \qquad (13)$$

It should be noted, however, that although the POT method is used here to estimate a 50-year return force for Ultimate Limit State (ULS) design considerations, the underlying wave conditions are derived from long-term average reanalysis data (mean $H_s \approx 0.54$ m). As such, the estimated ULS-level force primarily reflects rare high-end fluctuations within typical sea states, rather than forces associated with severe storm conditions. Future studies may incorporate design storm scenarios or higher percentile wave statistics to obtain more conservative estimates for ULS-level loading.

Figure 7 shows the empirical exceedance probability of the POT data (shown in blue) along with the fitted GPD model (shown as a red dashed line). The 50-year return level is

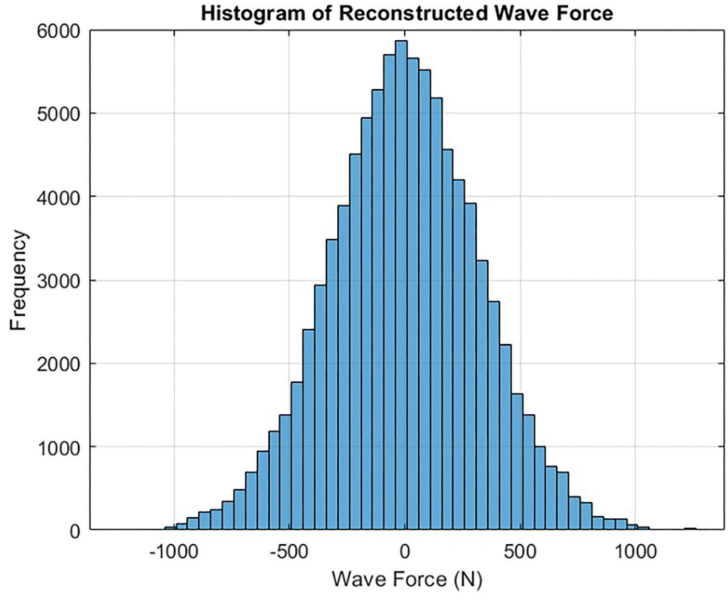

Figure 6. Histogram of reconstructed wave-induced force signal. The y-axis indicates the statistical frequency (count) of force amplitudes observed over the 10-year simulation period.

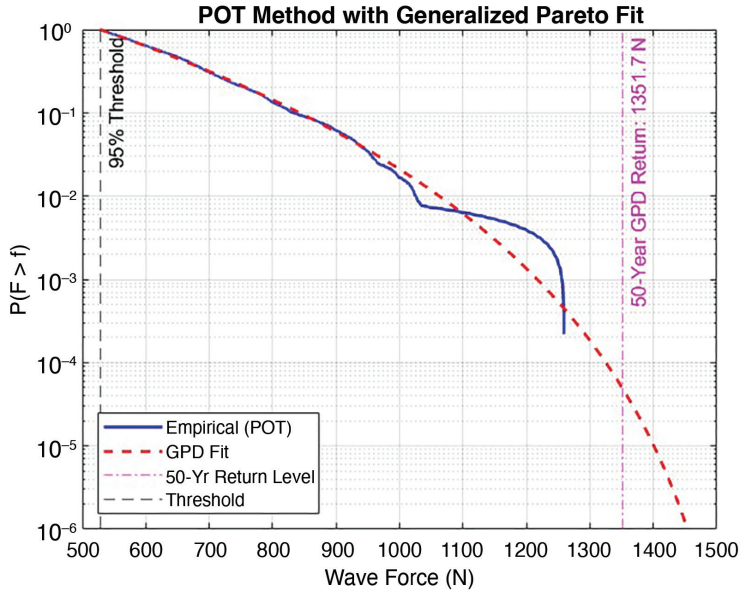

Figure 7. Exceedance probability plot of wave-induced forces above the 95th percentile threshold, fitted with a Generalized Pareto Distribution.

marked with a vertical magenta line. A strong agreement is observed in the upper tail, confirming the statistical validity of the model for extrapolating rare wave loading events. Minor stepwise features and curvature in the empirical curve at very low exceedance probabilities are attributed to the limited number of high-magnitude observations -a typical behavior in data-limited POT applications. This analysis highlights the advantage of using a continuous statistical model for reliable ULS-level force estimation under data-limited conditions.

To generalize the findings and facilitate comparisons across different monopile diameters, the wave force signal was normalized by the monopile diameter (D=2.5 m), resulting in a unit-diameter force representation (F_{norm} in N/m). The normalized signal exhibited a maximum of +503.63 N/m, a minimum of -490.63 N/m, and a standard deviation of 128.51 N/m. These values can be directly applied in parametric studies, load extrapolation efforts, and design evaluations involving geometrically scaled foundations, while remaining consistent with the assumptions of linear wave diffraction theory.

5. Conclusion

This study developed a numerical framework for reconstructing wave-induced forces on a monopile-supported offshore wind turbine located off the coast of Gökçeada in the northeastern Aegean Sea. A site-specific JONSWAP wave spectrum was calibrated using a decade of Mediterranean reanalysis data to represent the irregular sea states typical of fetch-limited environments.

To account for diffraction effects associated with the large monopile diameter, the MacCamy-Fuchs diffraction theory was applied. Spectral components with a non-dimensional wave number exceeding $ka>3$ were excluded to maintain theoretical consistency, resulting in an energy retention rate of approximately 97.5%. The filtered spectrum was then used to reconstruct a 10-year time-domain wave force signal via IFFT, capturing both short-term variability and long-term statistical trends.

The reconstructed signal exhibited a standard deviation of 321.27 N and a peak amplitude of 1259.08 N. To evaluate extreme loading, a POT analysis was conducted using the 95th percentile threshold, with exceedances fitted to a GPD. The resulting 50-year return force was estimated as 1351.7 N, providing a statistically consistent upper bound within the context of long-term average sea states (mean $H_s \approx 0.54$ m). Therefore, while the estimated force captures upper-bound fluctuations under typical wave conditions, it does not represent severe storm-induced loading that would be expected in conservative ULS design.

Spectral energy analysis showed that 88.4% of the wave energy was concentrated in the high-frequency band $f>0.3$ Hz, emphasizing the dominant role of short-period waves in monopile loading. For generalized application, the force signal was normalized by the monopile diameter, yielding a maximum unit-diameter force of 503.63 N/m.

This study focuses on the reconstruction of long-term, realistic wave-induced force histories on offshore monopile foundations in data-limited, fetch-limited regions by

relying solely on reanalysis wave data and diffraction-based modeling. Although previous studies have employed spectral wave models or diffraction theory independently, the integration of these approaches for time-domain force reconstruction under typical sea conditions remains limited-particularly in semi-enclosed basins such as the Aegean Sea. Addressing this gap, the present study introduces a physically consistent and scalable framework that combines a site-specific, validated JONSWAP spectrum with MacCamy-Fuchs diffraction theory and randomized-phase IFFT. This novel approach enables the generation of statistically representative wave load histories without requiring in-situ measurements, offering a robust tool for structural design, fatigue assessment, and reliability analysis of offshore wind turbine foundations in regions with limited observational resources.

In addition, the validated force time series provides a foundation for further investigations into long-term structural performance, especially in the context of fatigue and probabilistic reliability. While the present study focuses on average sea states, future work may incorporate storm conditions or extreme wave events to support more conservative ULS design assessments.

Footnote

Financial Disclosure: The author declared that this study received no financial support.

References

[1] M. Argin, V. Yerci, N. Erdogan, S. Kucuksari, and U. Cali, "Exploring the offshore wind energy potential of Turkey based on multi-criteria site selection," Energy Strategy Reviews, vol. 23, pp. 33-46, Jan 2019.

[2] S. Tolun, S. Mentese, Z. Aslan, and M. A. Yukselen, "The wind energy potential of Gökçeada in the Northern Aegean Sea," Renewable Energy, vol. 6, no. 7, pp. 679-685, Oct 1995.

[3] N. Eskin, H. Artar, and S. Tolun, "Wind energy potential of Gökçeada Island in Turkey," Renewable and Sustainable Energy Reviews, vol. 12, no. 3, pp. 839-851, Apr 2008.

[4] S. Şişbot, Ö. Turgut, M. Tunç, and Ü. Çamdalı, "Optimal positioning of wind turbines on Gökçeada using multi-objective genetic algorithm," Wind Energy, vol. 13, no. 4, pp. 297-306, Apr 2009.

[5] M. D. Akyol, E. Şahin, and S. Güçlüer, "Technical feasibility of offshore wind power plant for Gökçeada region in Türkiye," in 2023 12th International Conference on Renewable Energy Research and Applications (ICRERA), pp. 1016-1020, Aug 2023.

[6] American Bureau of Shipping (ABS), Design standards for offshore wind farms, Final Report, Contract No. M10PC00105, U.S. Department of the Interior, Bureau of Ocean Energy Management, 2011.

[7] L. Sartini, L. Mentaschi, and G. Besio, "Sub-mesoscale wave height return levels on the basis of hindcast data: the North Tyrrhenian Sea," Coastal Engineering Proceedings, vol. 1, no. 34, p. 39, Oct 2014.

[8] U. P. A. Pillai et al. "Wind-wave characteristics and extremes along the Emilia-Romagna coast," Natural Hazards and Earth System Sciences, vol. 22, no. 10, pp. 3413-3433, 2022.

[9] A. S. Ibrahim, A. El-Molla, and H. G. I. Ahmed, "Long-term trends in significant wave heights in the Mediterranean as an indicator of climate change," Transactions on Maritime Science, vol. 13, no. 2, Oct 2024.

[10] Y. Fan, "Analysis of long-term changes in extreme waves in the northwest pacific over the past 60 years," The EGU interactive community platform [Preprint], 2025.

[11] Z. Li, Z. Wang, B. Liang, and X. Wang, "Experimental study on hydrodynamic performance and structural forces of curved and vertical front face pile-supported permeable breakwaters," Physics of Fluids, vol. 36, no. 11, Nov 2024.

[12] G. Napitupulu, A. Tarya, I. G. M. Y. Pratama, and I. S. Winardhie, "Variability analysis of significant wave heights and wind waves in Riau Archipelago Sea Part ALKI 1," Jurnal Pesisir Dan Laut Tropis, vol. 10, no. 3, pp. 341-355, Oct 2022.

[13] A. Aggarwal, M. A. Chella, A. Kamath, and H. Bihs, "Irregular wave forces on a large vertical circular cylinder," Energy Procedia, vol. 94, pp. 172-181, Sep 2016.

[14] S. P. León, J. H. Bettencourt, and N. Kjerstad, "Simulation of irregular waves in an offshore wind farm with a spectral wave model," Continental Shelf Research, vol. 31, no. 15, pp. 1541-1557, Oct 2011.

[15] S. Kalvig, E. Manger, B. H. Hjertager, and J. B. Jakobsen, "Wave influenced wind and the effect on offshore wind turbine performance," Energy Procedia, vol. 53, pp. 202-213, 2014.

[16] P. Vlachogiannis, C. Peyrard, A. C. Pillai, M. Collu, and D. Ingram, "A comparison of the influence of using empirical or mathematically pre-defined wave energy spectra for tower base bending fatigue calculations," in Proceeding ASME 2023 5th International Offshore Wind Technical Conference, 2023.

[17] K. Spanoudaki, A. K. Chuchmala, and E. A. Varouchakis, "An integrated geostatistical and numerical modelling framework for spatiotemporal analysis of wave energy fields in the Aegean Sea," EGUsphere, 2025.

[18] F. Barbariol, A. Benetazzo, F. Bergamasco, S. Carniel, and M. Sclavo, "Stochastic space-time extremes of wind sea states: validation and modeling," in Proceeding ASME 2014 33rd International Conference on Ocean, Offshore and Arctic Engineering, vol. 8B, 2014.

[19] B. Xie, X. Ren, X. Jia, and Z. Li, "Research on ocean wave spectrum and parameter statistics in the northern South China Sea," in Proceeding Offshore Technology Conference, Houston, TX, USA, May 2019.

[20] Copernicus Marine Service, Product User Manual for Mediterranean Sea Waves Reanalysis (MEDSEA_MULTIYEAR_WAV_006_012), Issue 2.4, Mercator Ocean International, 2024. [Online]. Available: https://marine.copernicus.eu

[21] K. Hasselmann et al., "Measurements of wind-wave growth and swell decay during the Joint North Sea Wave Project (JONSWAP)," Ergänzungsheft zur Deutschen Hydrographischen Zeitschrift, A8, Hamburg: Deutsches Hydrographisches Institut, 1973.

[22] R. C. MacCamy, and R. A. Fuchs, Wave forces on piles: a diffraction theory, Technical Memorandum No. 69, Beach Erosion Board, U.S. Army Corps of Engineers, 1954.

[23] R. G. Dean, and R. A. Dalrymple, Water wave mechanics for engineers and scientists, vol. 2. World Scientific, 1991.